ELSEVIER

Solar Energy Materials & Solar Cells 71 (2002) 375–385

Solar Energy Materials & Solar Cells

www.elsevier.com/locate/solmat

Spectral effects on amorphous silicon solar module fill factors

Ricardo Rüther[a,*], Gerhard Kleiss[b], Kilian Reiche[c]

[a] *Universidade Federal de Santa Catarina, Caixa Postal 476, 88040-900, Florianopolis–SC, Brazil*
[b] *Shell Solar Deutschland Vertrieb GmbH, Shell Solar Zentrum Ost (SSDV–CME), Schillstr. 9, D-10785 Berlin, Germany*
[c] *The World Bank—Energy Unit, 1818 H Street NW, Washington, DC, 20433 USA*

Abstract

The outdoor operation and monitoring of amorphous silicon (a-Si) solar modules present unique features when compared to the more traditional and quite well understood operation of the crystalline silicon (c-Si) technology. The peculiarities of a-Si contrast to such extent with those of c-Si solar cells that in the field, while the former performs better during summer, the latter is more efficient in winter. Concepts usually applied to describe phenomena in c-Si devices are often inadequate to describe the performance of a-Si cells. When looking at module performance, the fill factor (FF) can be regarded as one of the characteristic photovoltaic quantities of major interest. Under outdoor illumination, cells are seasonally exposed to different solar spectral contents and intensities, which vary considerably from summer to winter. The FF depends on both the quality (spectrum) and quantity (irradiation) of the incident light. In this context, we report results showing spectral effects on the FF of amorphous silicon solar modules deployed outdoors. While "blue" spectra improved the FF of a-Si devices, the contrary was observed for "red" spectra. The voltage-dependent spectral response of a-Si devices is also described and quantified. Our results reveal that a-Si modules can perform quite well at low irradiations and mainly diffuse spectra. We, thus, conclude that in system sizing programmes, the performance of a-Si modules should be treated more precisely with respect to spectra, to reveal their true operational characteristics and advantages.

Keywords: Amorphous silicon; Fill factor; Spectral effects

*Corresponding author. Tel.: +55-48-331-5174; fax: +55-48-234-1519.
E-mail address: ruther@mbox1.ufsc.br (R. Rüther).

0927-0248/02/$ - see front matter
PII: S0927-0248(01)00095-2

1. Introduction

The first commercially available hydrogenated amorphous silicon (a-Si:H, or simply a-Si) solar modules, produced in the early 1980s [1], were optimised for indoor illumination, for low-power consumer applications like pocket-calculators and watches. This development took place, among other reasons, because of the possibility of producing low cost, monolithic, integrated-type, solar modules (in these applications they are usually intended for displacing or recharging 1.5–3 V batteries drawing very low currents). Moreover, the spectral response of a-Si presents an excellent match to the spectral content of room-light, making the amorphous cells in these applications actually more efficient photovoltaic (PV) converters than their crystalline silicon (c-Si) counterpart [1]. In these applications the light-induced degradation effect (Staebler–Wronski effect [2]) peculiar to a-Si is negligible and the deterioration of electrical parameters with exposure-time is not a matter of concern. However, amorphous silicon and its related alloy thin film technologies have evolved to a stage such that large-area solar modules are at present being more and more utilised to generate electrical power outdoors. Outdoor conditions depend on site location and time (on both a daily and yearly basis), and are therefore much less uniform than indoor conditions. Under outdoor conditions, the particular characteristics of a-Si contrast to such extent with those of c-Si that while a-Si solar cells perform better during summer months, c-Si cells are generally more efficient PV converters in winter. This seasonal effect in output performance has been extensively reported lately, and its causes have been assigned to either thermal annealing effects, spectral effects, or both [3–9]. The constant changing outdoor irradiance, temperature and spectral conditions strongly affect the performance of a-Si devices. Temperature coefficients of power for a-Si solar cells are much smaller than those presented by c-Si devices, another important contrast between the two PV technologies.

When evaluating module performance, the fill factor (FF) can be regarded as one of the characteristic PV quantities of major interest. The measurement and precise determination of the FF in a-Si, however, is not a trivial task. There exist similar problems, when the attempt is made to predict exactly the outdoor performance of a-Si modules as necessary for system sizing simulations. Light-induced degradation directly affects the FF of the amorphous silicon cells [10,11]. In contrast to the c-Si material, due to the amorphous structure of a-Si, there does not exist "one" a-Si, and different module types exhibit different performance profiles, since the a-Si material structure itself is conditioned by film-deposition conditions and film-deposition technology. This may in fact be a contributory cause for the somehow unexpected results reported by researchers at NREL [9], which indicate that multi-junction a-Si devices operated in the field present a higher degree of light-induced degradation as compared to single-junction a-Si solar modules.

The usual concept of treating spectral effects in crystalline devices does not hold for a-Si cells. Carrier lifetimes and mobilities in a-Si are much smaller than those in c-Si. Since the field-driven carrier transport plays a major role in a-Si solar cells, where the electric field is extended over virtually the whole device, the location of

carrier generation is of great importance for device performance. Different incident spectra (e.g. "blue" diffuse radiation in comparison with "red" direct irradiation) will produce varying generation profiles inside the cell. In amorphous silicon solar cell modelling, several approaches (e.g. the DICE method [12]) explore this fact to yield spatial resolution of the cell's field distribution. In more general terms, the spectral response curve of a-Si devices is a function of wavelength, bias voltage (i.e. the operation point of the cell), and bias light. As a consequence, neither the concept of spectral mismatch correction used in the calibration of a-Si modules nor the crystalline-style treating of spectral effects for system sizing will generally hold for a-Si devices. In this paper, we present experimental evidence for this effect, which is specific to a-Si devices deployed outdoors, and report on spectral effects on the FF of a-Si solar modules. The effect of the voltage-dependent spectral response of a-Si solar cells is also described and quantified.

2. Theory

The spectral effect on crystalline silicon devices is usually treated as a mismatch of the short circuit current (I_{sc}):

$$I_{sc} = \int E(\lambda) s(V = 0\,V, \lambda)\,\mathrm{d}\lambda \tag{1}$$

with respect to the total irradiation (G) as measured by integrating sensors like pyranometers,

$$G = \int E(\lambda)\,\mathrm{d}\lambda. \tag{2}$$

Assuming that linear superposition holds and that the spectral response of the solar cell does not vary with respect to the point of operation, the ratio between I_{sc} for the standard AM1.5 spectrum (measured at $1000\,\mathrm{W\,m^{-2}}$) and the I_{sc} for an arbitrary spectrum $E(\lambda)$ extrapolated to $1000\,\mathrm{W\,m^{-2}}$ is the spectral mismatch factor. This I_{sc}-mismatch can be used to estimate the effect of varying spectra on the cell and is known to be particularly large for wide bandgap materials like a-Si [13]. Often, a performance modelling with respect to irradiation (a $\eta(G)$ relation) is included to yield a more precise prediction of spectral effects [4].

However, in amorphous silicon solar cells, the proposition of the non-dependence of $s(\lambda)$ on the operating voltage does not hold. It is known that in p-i-n structures a typical blue-dispersion of the spectral response occurs for higher bias voltages [14]. Since the field-driven transport is the dominant mechanism with respect to diffusion, and since the electrical field is extended over practically the whole cell, the generation profile inside the cell produces a feedback on the internal quantum efficiency. In a-Si cell modelling, one takes advantage of this effect by application of the DICE method [12,15,16] to yield for a spatially resolved description of the field distribution inside the cell.

In the scope of this paper, the major consequence of this is the need for treating two different spectral effects, at I_{sc} and at the maximum power point (MPP) to yield

the FF. The latter effect can be estimated by calculating the current at MPP (I_{MPP}) with a bias-dependent spectral response at V_{MPP}:

$$I_{MPP} = \int E(\lambda)s(V_{MPP,\lambda})\,d\lambda. \tag{3}$$

The spectral effect on the FF reported in this paper may be estimated by the ratio of I_{MPP} and I_{sc} calculated according to Eqs. (1) and (3).

3. Experimental

Several commercial a-Si modules (single-junction p-i-n technology) have been exposed outdoors and measured continuously at outdoor measurement facilities in Freiburg, Germany (latitude: 48°N) and Cadarache, France (latitude: 43°N). The modules were oriented southwards and tilted by the geographical latitude. Frequency of measurement (complete $I-V$ curve) was every 4 min for the Freiburg site, and every 12 min for the Cadarache site. Meteorological data were simultaneously acquired at both sites. Monitoring of irradiation was carried out as follows: For the Freiburg site, both a clear glass pyranometer (CM11 Kipp&Zonen) and a filtered pyranometer (RG805 filter on a PSP Eppley pyranometer) were used. For the Cadarache site, the global irradiation was measured with a clear glass pyranometer, whereas the diffuse irradiation was monitored with a shadow band pyranometer (both CM11 Kipp&Zonen). We define the "redness index" (used for the Freiburg site) as the ratio of the irradiances measured by the filtered glass pyranometer and the clear glass pyranometer (both mounted at the plane-of-array, POA); and the "diffuse fraction" (used for the Cadarache site) as the ratio of the shadow band pyranometer and the clear glass (global) pyranometer, both mounted at POA. It is worth mentioning that while a high redness index indicates a "redder" spectrum, a high diffuse fraction indicates a "bluer" spectrum. Module temperatures were measured on the backside of the modules by means of either platinum resistance (PT100) or thermocouple sensors.

The continuous outdoor measurements started in summer, and the results presented in this paper refer to periods after the first six months of deployment outdoors (August–January). With respect to degradation, although stabilisation had at that stage not yet been reached, degradation effects can be considered far less important than in the first months of outdoor exposure.

4. Results and discussion

We now present and discuss some experimental and simulation results related to the spectral effects on the FF of a-Si solar modules.

4.1. Experiment

Fig. 1 shows the measured FF versus I_{sc} for an a-Si module measured at the Cadarache site after the first six months outdoors. The data points are plotted as measured, no temperature correction has been applied. An interesting phenomenon occurred for irradiation levels below $500\,W\,m^{-2}$ (corresponding to I_{sc} of less than 0.25 A in the graph): a large scatter in FF was found, that could not be explained by means of temperature correction as can be seen from Fig. 2. Fig. 2 shows the same data points shown in Fig. 1, plotted versus the module temperature (T_{module}). No correlation between FF and temperature can be found. However, the two scatter clouds correspond to the regimes of high and low irradiations as shown in Fig. 1. In this respect, it is important to note that the performance of crystalline silicon modules observed during the same period did not exhibit this effect, as can be seen in Fig. 3, which shows the FF versus I_{sc} plots for a c-Si module measured at the Cadarache site for the same period. This is due to the fact that when the FF of a c-Si module is plotted versus I_{sc}, spectral effects are already eliminated ($I_{sc} = \int E(\lambda)s(\lambda)\,d\lambda$) and the remaining effect of temperature can be easily corrected.

The explanation for the large scatter shown in Fig. 1 can be found by relating the graph to information dependent on spectrum. The diffuse fraction (ratio between diffuse and global irradiation) may serve as a tool, since large diffuse fractions indicate "bluer" spectra (as compared to the standard spectrum). For the season and site locations reported herewith, as far as small diffuse fractions are concerned, one encounters "red" spectra for low irradiations on clear days (i.e. for a low position of

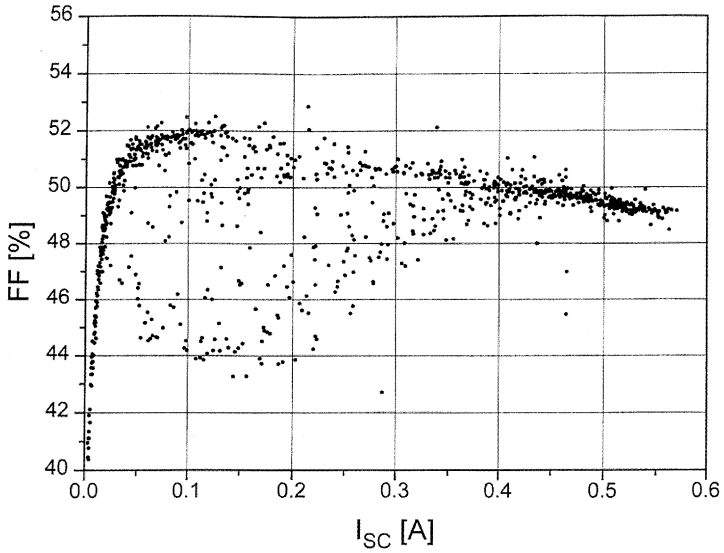

Fig. 1. The fill factor FF as a function of I_{sc} for an amorphous silicon PV module measured during January at the Cadarache site (latitude: 43°N). Points are shown as measured, no temperature correction has been applied.

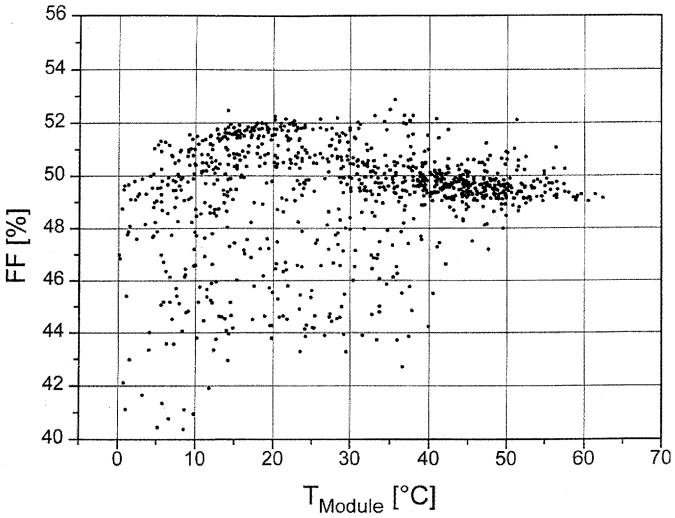

Fig. 2. The fill factor FF as a function of module temperature T_{module} for an amorphous silicon PV module measured during January at the Cadarache site (latitude: 43°N).

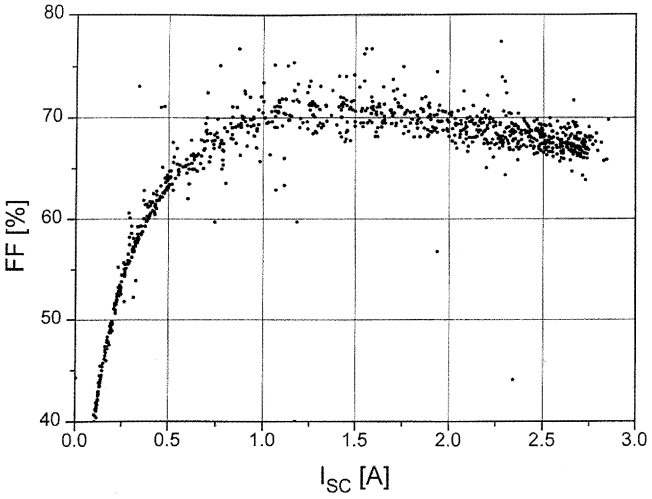

Fig. 3. The fill factor FF as a function of I_{sc} for a crystalline silicon PV module measured during January at the Cadarache site (latitude: 43°N). Points are shown as measured, no temperature correction has been applied.

the sun in the early morning or late afternoon), and spectra that are more similar to the standard spectrum at solar noon for large irradiations.

In Fig. 4, the influence of spectrum on the FF is depicted exploiting two different diffuse fractions. The largest FFs are encountered for "blue" spectra (large diffuse

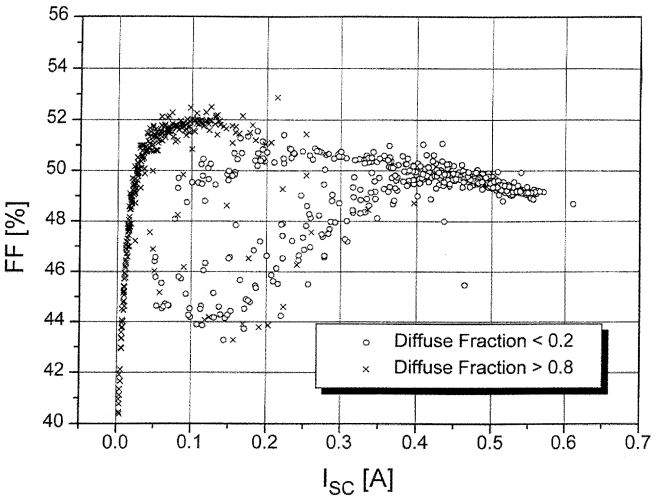

Fig. 4. The fill factor FF as a function of I_{sc} for an amorphous silicon PV module (same data as in Fig. 1) for two different diffuse fractions ("redder" and "bluer" spectra).

fractions, shown as crosses in the graph) for $0.05\text{A} < I_{sc} < 0.1$, whereas the logarithmic decrease in V_{oc} limits the FF below $I_{sc} = 0.05\,\text{A}$. The small diffuse fractions (open circles in the graph) encompass spectra similar to the standard spectrum for high irradiations (at around solar noon) and the "red" spectra (in the afternoon and morning hours) responsible for the observed large scatter from Fig. 1. To summarise, the effect of "blue" spectra is to increase the FF, while a red shifted spectrum decreases the FF.

The transparent conducting oxide (TCO) which carries the photogenerated current in a-Si solar cells represents a limitation to the device's FF. Sheet resistivities of commonly used TCO materials (e.g. SnO_2, ZnO) are such that losses become large at high solar irradiances. It could be argued that TCO limitations could be responsible for the reduced FF at higher I_{sc} as shown in Fig. 4. The figure also shows, however, that a strong reduction in FF can also occur at low diffuse fractions (i.e. red shifted spectra) and low I_{sc} (low irradiances), where TCO sheet resistance should not represent a limitation.

Fig. 5 shows a plot of the FF as a function of I_{sc} for an a-Si solar module measured at the Freiburg site (same module type, outdoor exposure time and time of the year measurements as for the Cadarache module shown in Figs. 1, 2 and 4). Here, we used the redness index previously defined, and the same trend shown in Fig. 4 can be seen, with "bluer" spectra leading to larger FF.

4.2. Simulation

In order to resolve the difference in the spectral performance of a-Si modules at MPP with respect to I_{sc}, a simulation was performed with the spectral response

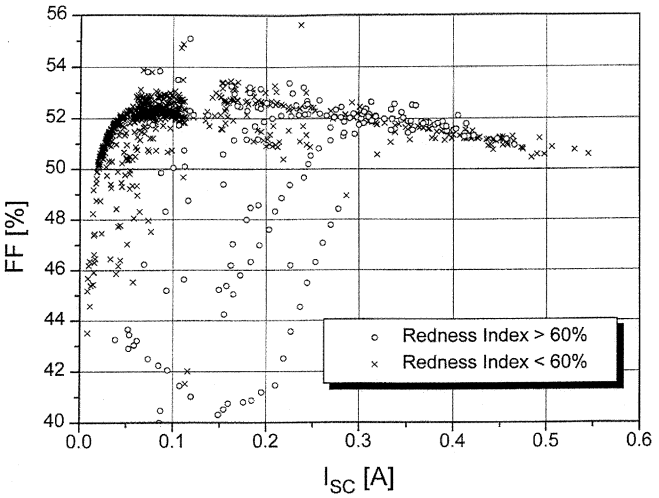

Fig. 5. The fill factor FF as a function of I_{sc} for an amorphous silicon PV module measured during January at the Freiburg site (latitude: 48°N), for redness indexes higher ("redder" spectra) and lower ("bluer" spectra) than 60%. Points are shown as measured, no temperature correction has been applied.

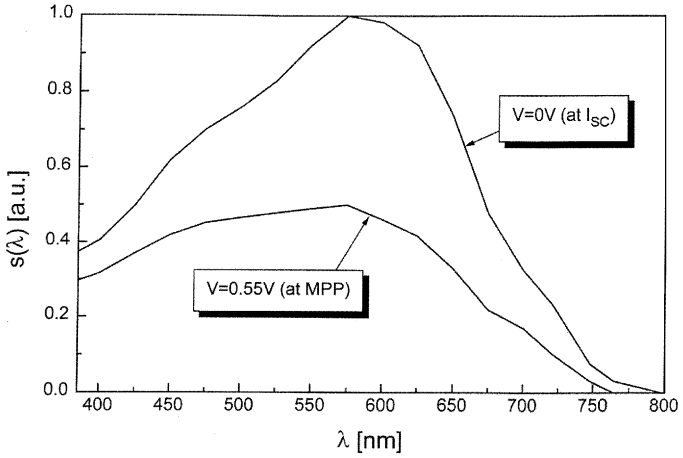

Fig. 6. Spectral response for different operation voltages (adapted from [17]). Maximum power point (MPP) selected as fixed voltage operation at $V = 0.55\,\mathrm{V}$.

curves taken from Bruns [17] depicted in Fig. 6. As can be seen, a typical blue dispersion towards higher operation voltages yields a shift of the maximum of $s(\lambda)$ for the fixed operation voltage $V = 0.55\,\mathrm{V}$, a typical maximum power voltage of an a-Si cell. Thus, I_{sc} can be obtained by integrating the upper curve in Fig. 6 with the incident spectrum, whereas the current at MPP (which is less than I_{sc}) is estimated by integrating the lower curve (at $V = 0.55\,\mathrm{V}$) with the incident spectrum. In this

approximation, we focused only on the ratio of the so-calculated currents and the case of fixed voltage operation, thus neglecting the dependence of the MPP voltage on the incident irradiation. The dependence of the FF on temperature and integral irradiation (as included in the measurements, Figs. 1–5) were neglected as well.

Fig. 7 exhibits the ratio of the calculated currents at $V = 0\,\mathrm{V}$ (I_{sc}) and $V = 0.55\,\mathrm{V}$ (near MPP) with respect to G for a yearly spectral database [18] for the geographical location of Freiburg, Germany. As can be seen in the graph, the scatter for low irradiations ($< 300\,\mathrm{W\,m^{-2}}$) is considerable (10–15%), corresponding to the strongly varying spectral situations between "blue" spectra (mainly diffuse irradiation) and "red" spectra (direct irradiation). For higher irradiation levels ($> 800\,\mathrm{W\,m^{-2}}$), one encounters a smaller scatter (3%), since mainly direct radiation spectra contribute to this regime, which are more similar when compared to the low irradiation regime. Again, it is noteworthy that no scatter would be expected in the case of crystalline devices, and that this effect occurs only due to the operation voltage-dependent spectral response of a-Si cells.

When considering diffuse radiation a second effect besides the "blue" spectrum has to be taken into account. Due to the nearly isotropic inclined on the module surface the maximum of the generation profile is shifted closer to the front surface of the cell. Thus, both effects add constructively.

5. Summary and conclusions

Spectral effects on the FFs of a-Si solar cells have been reported. "Blue" spectra have been shown to be beneficial for the FF of the devices investigated, whereas

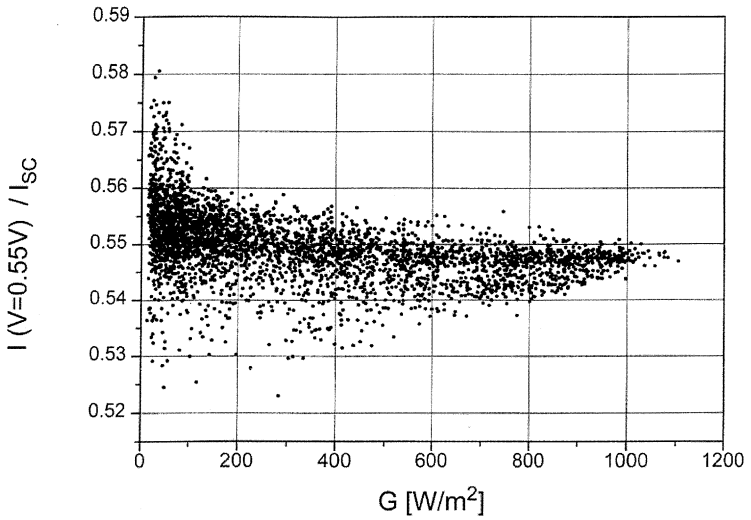

Fig. 7. Hourly ratio of the currents calculated with the $s(\lambda)$ (adapted from [17]) for $V = 0\,\mathrm{V}$ (I_{sc}) and $V = 0.55\,\mathrm{V}$. The simulation was performed for a meteorological data set acquired during one year in Freiburg [18].

"red" spectra decreased their FF. This effect adds up to the spectral effect of a-Si at $V = 0\,\mathrm{V}$ (I_{sc}) often reported. The maximal deviations are in the order of 10%, which add to the maximum effect as reported at I_{sc} of typically 15% [13]. The effect of the voltage-dependent spectral response of a-Si solar cells has also been reported and quantified from outdoor measurements.

For a-Si module calibration at irradiations $G > 900\,\mathrm{W\,m^{-2}}$, one has to take into account an additional uncertainty of at least 3% in P_{max} (i.e. in η), due to spectral effects, even if a conservative mismatch correction for the short circuit current is performed. In system sizing programmes, the performance of a-Si modules should be treated more precisely with respect to spectra. This will reveal the good performance of a-Si modules at low irradiations with mainly diffuse spectra. Within the German 1000-Roofs Programme, a-Si modules have demonstrated better than expected performances [19], with performance ratios (PR)[1] exceeding 82% in the first year (the best PR among all the other c-Si installations within the programme) and dropping to a still higher than expected 75.4% in the second year (still higher than most of the c-Si installations).

With the emergence of thin film PV for outdoor applications, assessment criteria taking into account the technology's peculiarities need to be established. Compared to the more mature technology of c-Si PV, either single or polycrystalline, a-Si presents contrasting peculiarities, which in the field, under real outdoor conditions, can result in surprising shifts from the expected performance as we have shown.

Acknowledgements

The authors are grateful to Ph. Ragot for valuable discussion and measurement support, and to NAPS France for providing modules for testing. Work reported in this paper has been supported by BWT under contract number 0328650F, and was carried out at the Fraunhofer Institute for Solar Energy Systems (Fraunhofer ISE) in Germany and at GENEC—C.E. Cadarache in France. G. Kleiss gratefully acknowledges financial support from the German Academic Exchange Service DAAD for enabling research at GENEC, C.E. Cadarache. R. Rüther acknowledges with thanks the support of the Alexander von Humboldt Foundation (AvH), the Fraunhofer Institute for Solar Energy Systems (Fraunhofer ISE), and the Brazilian Research Council (CNPq).

References

[1] Y. Kuwano, T. Imai, M. Ohnishi, S. Nakano, Proceedings of the 14th IEEE Photovoltaic Special Conference, San Diego, 1980, p. 1408.

[1] In the German 1000-Roofs Programme, the performance ratio (PR) is defined as the ratio of the AC energy output (EAC) and the rated efficiency (ηSTC) times the total solar radiation incident on the module's surface (ES), PR = 100[EAC/(ηSTC ES)]%. This first systematic grid-connected photovoltaic programme, precursor of the current 100.000-Roofs Programme, installed some 2250 roof-mounted PV installations, most of which consist of c-Si modules whose PR averaged 65.3% in 1994 [19].

[2] D.L. Staebler, C.R. Wronski, Appl. Phys. Lett. 31 (1977) 292.
[3] H.S. Costa, P. Ragot, D. Desmettre, Sol. Energy Mater. Sol. Cells 27 (1992) 59.
[4] G. Kleiss, K. Bücher, A. Raicu, K. Hiedler, Proceedings of the 11th European Photovoltaic Solar Energy Conference, Montreux, 1992, p. 578.
[5] T. Yanagisawa, Microelectron. Reliab. 35 (1995) 183.
[6] K. Takahisa, K. Nakamura, S. Nakazawa, Y. Sugiyama, J. Nose, S. Igari, T. Hiruma, Sol. Energy Mater. Sol. Cells 34 (1994) 485.
[7] S. Guha, J. Uang, A. Banerjee, T. Glatfelter, K. Hoffman, X. Xu, Sol. Energy Mater. Sol. Cells 34 (1994) 329.
[8] R. Rüther, J. Livingstone, Sol. Energy Mater. Sol. Cells 36 (1994) 29.
[9] B. von Roedern, B. Kroposki, T. Strand, L. Mrig, Proceedings of the 13th European Photovol. Solar Energy Conference, Nice, 1995, p. 576.
[10] G. Kleiss, K. Bücher, P. Ragot, M. Chantant, Proceedings of the First World Conference on Photovoltaic Energy Conversion, Hawaii, 1994, p. 531.
[11] P. Ragot, A. Chenevas-Paule, H.S. Costa, D. Desmettre, E. Rossi, H. Ossenbrink, R. van Steenwinkel, Proceedings of the Tenth European Photovoltaic Solar Energy Conference, Lisbon, 1991, p. 403.
[12] T. Takahama, M. Isomura, S. Tsuda, H. Tarui, Y. Hishikawa, N. Nakamura, Y. Nakashima, T. Matsuoka, H. Nishiwaki, M. Ohnishi, S. Nakano, Y. Kuwano, Jpn. J. Appl. Phys. 25 (1986) 1538.
[13] S. Nann, K. Emery, Sol. Energy Mater. Sol. Cells 27 (1992) 189.
[14] J. Bruns, S. Gall, H.G. Wagemann, Proceedings of the 22nd IEEE Photovoltaic Special Conference, Las Vegas, 1991, p. 1323.
[15] R. Saeng-Udom, W. Kusian, B. Bullemer, Proceedings of the 11th European Photovoltaic Solar Energy Conference, Montreux, 1992, p. 609.
[16] C. Hof, D. Fischer, A.V. Shah, Proceedings of the 12th European Photovoltaic Solar Energy Conference, Amsterdam, 1994, p. 132.
[17] J. Bruns, Ph.D. Thesis, Technische Universität, Berlin, 1993.
[18] H.R. Wilson, M. Hennies, Sol. Energy 42 (1989) 273.
[19] K. Kiefer, V. Hoffman, Annual Report of the 1000-Roofs Program, Fraunhofer-Institut für Solare Energiesysteme, 1994.